Experimental evidence on the nonlocality of the electron distribution function

U. Kortshagen
Institute of Experimental Physics II, Ruhr-Universität Bochum, 44780 Bochum, Germany
(Received 8 November 1993)

In view of the increasing interest in the modeling of complete plasma devices the influence of the spatial inhomogeneity on the formation of the electron distribution function (EDF) is attracting growing attention. In this paper the radial dependence of the EDF has been investigated experimentally in a cylindrical high frequency (hf) sustained plasma by means of Langmuir probe diagnostics. As a conclusion of the experimental results the electron distribution function can be considered as a spatially homogeneous function of the total energy (i.e., kinetic plus potential energy) of the electrons. The correspondence between the experimental result and the basic ideas of the so-called "nonlocal approach" for solving the spatially inhomogeneous electron Boltzmann equation is pointed out. The main simplification achieved by the nonlocal approach is that the EDF is obtained from a spatially averaged kinetic equation. Nevertheless no information about the spatial variation of the distribution of the kinetic energies of the electrons is lost. A quantitative comparison between a self-consistent plasma model for the considered hf surface wave sustained plasma, based on the nonlocal approach, and measured EDF's is performed. For sufficiently small pressures good quantitative agreement is found. The deviations at higher pressures are attributed to the influence of stepwise ionization, which is only considered in a rough manner in the present investigation.

PACS number(s): 52.40.Hf, 52.70.Ds, 52.80.Pi, 51.50.+v

I. INTRODUCTION

As a recent development in the modeling of low pressure discharges the influence of spatial inhomogeneities on the formation of the electron distribution function (EDF) has attracted increasing interest [1–18]. In particular, with a view on the modern trend of describing complete plasma devices by models involving one or two spatial dimensions (e.g., [19,20]) obviously the consideration of the spatial dependence of the EDF is inevitable. From various types of discharges it is well known that homogeneous plasma models, making use of the spatially homogeneous Boltzmann equation and assuming an equilibrium of the EDF with the local electric field strength, may lead to erroneous results for the EDF. Thus, for instance, the calculation of the EDF in the capacitively coupled rf discharge requires an appropriate inclusion of the nonlocal heating of electrons in the strongly inhomogeneous rf field and via the oscillating sheaths (see, e.g., [3,11]). These nonlocal effects can hardly be accounted for in a homogeneous model.

Different techniques have been developed to include the spatial inhomogeneity in the modeling of the electron kinetics. The kinetic equations resulting from the spatially inhomogeneous Boltzmann equation have been solved directly by different approaches in Refs. [1–3]. The solution of the Boltzmann equation has been performed in a statistical way by the use of Monte Carlo [4–7] or particle in cell methods (combined with Monte Carlo) [8–13]. Direct solutions of the Boltzmann equation have been performed using convective schemes [14–17] or flux corrected transport algorithms [18]. However, with respect to models involving two or even three spatial dimensions, all these techniques become computationally very intense.

A simple and very effective approach to the inhomogeneity problem has been proposed by Bernstein and Holstein [21] and Tsendin [22]. This method presents a significant simplification to the complete solution of the spatially inhomogeneous Boltzmann equation in the regime of low pressures, when the energy relaxation length of electrons is large compared to the scale lengths of spatial inhomogeneity. The main idea of this approach is the description of the EDF of the whole spatially inhomogeneous system by a single distribution function of total energy. Nevertheless, although obtained from a spatially averaged kinetic equation, in this single function the spatial information is still fully included, since the EDF of total energy together with the space charge potential unambiguously determines the distribution function of kinetic energy for every spatial position [21–23]. Of course the (dc) ambipolar space charge potential and the high frequency (hf) electric field intensity (profile) have to be calculated self-consistently within this approach.

In a recent publication [24] the nonlocal approach has been applied to the situation of an overdense, microwave sustained plasma in cylindrical geometry, such as, for example, a surface wave produced plasma. It has been demonstrated that measurements of the radial distribution of spectral line intensities [25] could be much better described by a nonlocal than by a homogeneous, local model (homogeneous Boltzmann equation and assumption of equilibrium of the EDF with the local electric field). However, a comparison with line intensity measurements is only a more or less indirect indication on the validity of the nonlocal model. A direct proof of this model can only be obtained by the radially resolved measurement of the EDF. This topic is addressed in the

present investigation. Radially resolved probe measurements of the EDF in a surface wave produced plasma at 190 MHz are performed in argon, neon, and helium. The results are compared to the predictions of a nonlocal model, which has been improved compared to the one presented in Ref. [24].

This paper is organized as follows: in order to clarify the correspondence between the experimental observations and the basic ideas of the nonlocal approach, in Sec. II the experimental setup and the qualitative nature of the experimental results are described. The physical foundation of the nonlocal approach as well as the basic equations of the model employed are discussed in Sec. III. A quantitative comparison between experimental and theoretical results is given in Sec. IV while in Sec. V the conclusions are presented.

II. EXPERIMENTAL SETUP AND OBSERVATIONS

The experimental setup, which has been used for the present investigation, is depicted in Fig. 1. The plasma is excited and sustained by a propagating surface wave at 190 MHz. The wave is launched via a surfatron [26]. For surface wave plasmas it is well known that usually the hf component of the electric field is axially directed inside the plasma. Only in a thin layer close to the wall may the radial component contribute significantly in sustaining the plasma. The glass discharge tube (Duran, $\varepsilon_g = 4.7$) has an inner diameter of 28 mm and an outer diameter of 32 mm. A radially movable probe is inserted from the end of the discharge tube in axial direction. It consists of a tungsten wire of 6 mm length and a radius of 50 μm. The probe holder is a ceramic tube with an outer radius of 200 μm. Close to the measuring probe a second, floating potential reference probe is mounted, which is moved simultaneously with the measuring probe. The counter electrode for the probe circuit is placed inside the surfatron. The described triple probe setup is used to avoid the problems which may arise with an asymmetrical double probe system (see, e.g., [27]): namely, an insufficient area ratio between probe and

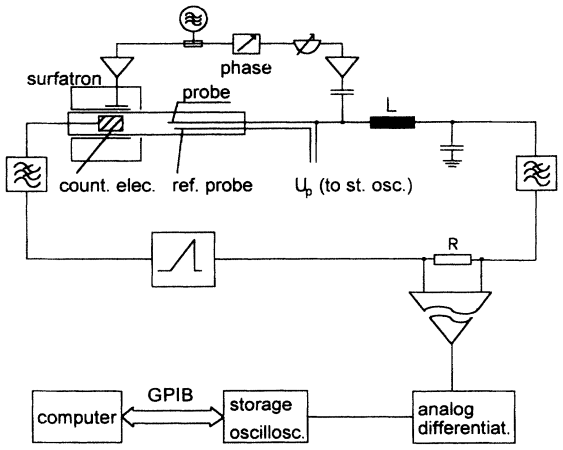

FIG. 1. Experimental setup for the measurements of the EDF and for the compensation of hf fluctuations of the plasma potential.

counter electrode [28,29] or a nonconstant voltage drop over the plasma resistance or the sheath of the counter electrode [30]. The hf fluctuation of the plasma potential is compensated by the use of an active method [31]. A compensating signal, which is adjustable in phase and amplitude, is coupled to the probe capacitively. By driving the probe simultaneously with the hf fluctuations of the plasma potential, the voltage drop across the probe sheath is kept constant in time.

The EDF of kinetic energy $f_0(u)$ can be obtained from the second derivative of the Langmuir probe characteristic in the range of the electron retardation current ($U \leq U_s$, with U the probe potential and U_s the plasma potential) [32]:

$$f_0(u) \propto \frac{d^2 I_p}{dU_p^2} . \tag{1}$$

Here I_p is the probe current and $U_p = U_s - U$ is the probe potential referenced to the plasma potential. Usually the zero crossing of the second derivative is considered to be the dc value of the plasma potential at the probe position (e.g., [33,34]). The kinetic energy u (in volts) in Eq. (1) is simply equal to U_p. Thus measured electron kinetic energies increase when the probe voltage is getting more negative with respect to the plasma potential.

In the present investigation a pulsed probe technique [33–35] is used, so that the primary experimental result is the second derivative with respect to time $d^2 I_p / dt^2$, which is obtained by the use of an analog twofold differentiating network. The voltage source is swept linearly in time. Unfortunately this does not necessarily imply that the voltage drop across the probe sheath U_p is also varying linearly. Many possible effects may disturb the linearity of $U_p(t)$: for instance, low frequency fluctuations, e.g., due to the electricity network, or a considerable nonconstant voltage drop across the plasma resistance and the sheath of the counter electrode. A possible nonlinearity of the probe voltage $U_p(t)$ is accounted for by the simultaneous measurement of the potential of the measuring probe and the floating potential of the reference probe. The potential difference between the measuring and the reference probe is assumed to be equal to U_p up to an additive constant, i.e., it is assumed that the difference between the floating potential of the reference probe and the plasma potential is constant. The second derivative of the probe current with respect to the probe voltage U_p is then obtained by [35]

$$\frac{d^2 I_p}{dU_p^2} = \left\{ \frac{d^2 I_p}{dt^2} \frac{dU_p}{dt} - \frac{dI_p}{dt} \frac{d^2 U_p}{dt^2} \right\} \left\{ \frac{dU_p}{dt} \right\}^{-3} . \tag{2}$$

This equation reduces to $d^2 I_p / dU_p^2 \propto d^2 I_p / dt^2$ only when the probe voltage U_p is strictly linear in time. The voltage source is swept within a time of typically 10 ms synchronized with the electricity net. The height of the voltage ramp is 60 V for helium and neon or about 40 V for argon. The bandwidth of the differentiating network is limited to 5 kHz, so that the effective energy resolution is of the order of 1 V. For the measurement of low energy electrons this resolution is insufficient [34] and should be

increased for future investigations. The current is measured by the voltage drop over a resistor (50–200 Ω), the signal is transferred by an isolation amplifier. All signals are recorded by a storage oscilloscope. The second derivatives are obtained as averages over 256 single measurements each. The electron densities are evaluated by integrating the measured EDF's (see [34]).

In the following typical characteristics of the experimental results should be pointed out. In Fig. 2 some typical measured second derivatives (i.e., EDF's of kinetic energy) at radial positions between 0 and 13 mm in argon are depicted. As explained above, the kinetic energy increases from the right limit of each curve, which corresponds to the zero crossing of the second derivative and thus to the zero of kinetic energy, to left. When moving from the axis towards the wall, the zero crossing shifts towards smaller values of the probe potential. Thus the potential difference related to the potential of the zero crossing on the axis is negative. This behavior, of course, mirrors nothing else than the variation of the dc ambipolar potential. The important experimental observation is that in spite of the shifts of the zero crossings of the individual curves, the high energy parts of all curves coincide, at least within the experimental accuracy. This behavior is best interpreted in terms of the total energy. At a distinct radial position the kinetic energy scale of the EDF is shifted exactly by the value of the ambipolar potential and thus by the value of potential energy of electrons (in volts) in this position as compared to the potential on the axis. Thus all curves can be considered as being plotted against one unique total energy scale (see Fig. 2). Following this idea, the coincidence of the measured EDF's implies that for some (sufficiently high) value of total energy the same amount of electrons is found in every radial position. In other words: *the EDF of total energy is independent of the radial coordinate.* However, at a radial position remote from the axis not the whole EDF of total energy is observable, but only that part with a total energy higher than the potential energy in this position. Electrons with a total energy less than this threshold value are not able to overcome the space charge potential. Thus the low energy part of the EDF is cut. In fact this cutting of the EDF is only qualitatively seen in Fig. 2, some depletion of the measured EDF's in comparison to the ideal shape is observed at low (kinetic) energies. However, it is well known that the experimental determination of the EDF is particularly sensitive to distortions in the vicinity of the zero crossing of the second derivative [34,36]. Possible sources of error may be the limited bandwidth of the differentiating network and some remaining miscompensation of the hf fluctuations of the plasma potential. In particular, the compensation of the radial component of the surface wave field, which is by $\pi/2$ out of phase with the axial component, is not possible by the employed active compensation method. Similar observations as in Fig. 2 have recently been reported by Godyak and Piejak in a capacitively coupled rf discharge [37], with a much better resolution of the low energy part of the EDF and an even more obvious demonstration of the cutting effect. Measurements with similar results have also been reported in [38,39].

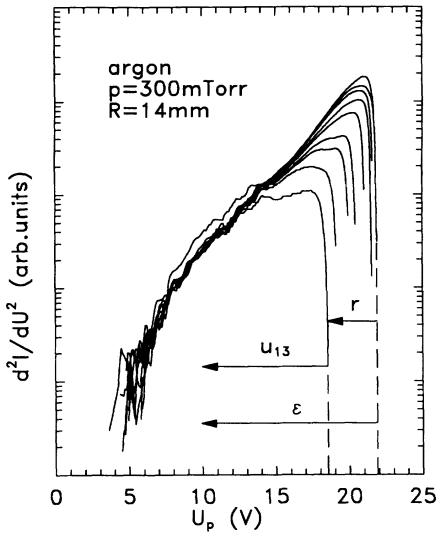

FIG. 2. Typical second derivatives measured at different radial positions: 0, 2, 4, 6, 8, 10, 11, 12, 13 mm (from right to left). u_{13} exemplifies the kinetic energy scale for the EDF (second derivative) at 13 mm, ε denotes the unique total energy scale for all measurements.

III. THE NONLOCAL KINETIC MODEL

A. Description of the model

Since the "nonlocal approach" is not very widely established up to now, a short review on the basic ideas should be given, in particular, in order to demonstrate the direct correspondence between the physical background of this approach and the experimental results discussed above. For a more detailed and exact discussion on the foundation of the nonlocal approach the reader is referred to the publications of Bernstein and Holstein [21] and Tsendin [22].

The starting point in the determination of the (isotropic part of the) EDF is the kinetic equation resulting from the spatially inhomogeneous Boltzmann equation after employing the Lorentz approximation [40] and assuming the time independence of the isotropic part of the EDF [40]. The kinetic equation is usually written in terms of a spatial coordinate (here the radius for cylindrical geometry) and the velocity or kinetic energy (e.g., [40]):

$$\frac{2}{3}\frac{e}{m_e}\frac{u^{3/2}}{\nu_m}\left[\nabla_r^2 F_0-\nabla_r\cdot\left[\mathbf{E}_s\frac{\partial F_0}{\partial u}\right]\right]+\frac{2}{3}\frac{e}{m_e}\frac{\partial}{\partial u}\left[\frac{u^{3/2}}{\nu_m}(-\mathbf{E}_s\cdot\nabla_r)F_0+\frac{u^{3/2}}{\nu_m}\left[|E_s|^2+\frac{|E_p|^2}{2}\frac{\nu_m^2}{\omega^2+\nu_m^2}\right]\frac{\partial F_0}{\partial u}\right]$$
$$+\frac{\partial}{\partial u}(u^{3/2}\kappa\nu_m F_0)=\sum_k[\nu_k(u)\sqrt{u}F_0(u)-\nu_k(u+u_k)\sqrt{u+u_k}F_0(u+u_k)]+S_{ee}\ . \quad (3)$$

The isotropic part of the EDF F_0 is normalized by $\int F_0(u,r)\sqrt{u}\,du = n_e(r)$. m_e is the electronic mass, $\mathbf{E}_s$ the dc space charge electric field, E_p the amplitude of the hf field, ν_m is the momentum transfer collision frequency, and ν_k the collision frequency of the kth inelastic process with the threshold energy u_k. The different terms in Eq. (3) account for (in the order of their appearance) spatial diffusion of electrons, the transport by the space charge field (second and third terms), the heating by the space charge and the hf electric field, the energy loss in elastic collisions, and the action of inelastic collisions and of the electron-electron collisions. The assumption of time independence of F_0 results in the inclusion of all frequency dependences in the definition of the effective electric field strength [41] [see fifth term of Eq. (3)]: $E_{\text{eff}}(u)=(E_p/\sqrt{2})\nu_m(u)/\sqrt{\nu_m^2(u)+\omega^2}$.

The situation addressed by the nonlocal approach is that of a discharge at sufficiently low pressure, so that the energy relaxation length of the electrons $\lambda_\varepsilon=\lambda_e\sqrt{\nu_m/(\kappa\nu_m+\nu^*)}$ [22] exceeds the discharge dimensions. Here λ_e is the electron mean free path, $\kappa=2m_e/M_a$ the energy transfer coefficient in elastic collisions with M_a the atomic mass, and ν^* the total inelastic collision frequency. This requirement is obviously most stringent in the energy range where inelastic collisions occur. Under these conditions electrons confined in the space charge potential (see Fig. 3) perform a diffusive motion with an (almost) constant total energy. Thus the total energy $\varepsilon=mv^2/2e-\Phi(r)$ in volts [with $\Phi(r)\le 0, \Phi(r=0)=0$] is a more suitable variable for the description of the EDF than the velocity or kinetic energy. By substitution one obtains from Eq. (3)

$$\frac{2e}{3m}\left[\frac{1}{r}\frac{\partial}{\partial r}\left[r\frac{u^{3/2}(r)}{\nu_m}\frac{\partial}{\partial r}F_0(\varepsilon,r)\right]+\frac{\partial}{\partial\varepsilon}\left[\frac{u^{3/2}(r)}{\nu_m}E_{\text{eff}}^2(r,u(r))\frac{\partial}{\partial\varepsilon}F_0(\varepsilon,r)\right]\right]=S_{ea}+S_{ee}\ . \tag{4}$$

The electron-atom collision term S_{ea} comprises elastic and inelastic collisions.

In particular, for the idealized case of collisionless motion of electrons in a confining space charge potential without accelerating electric field the EDF of total energy is obviously independent of the spatial coordinate [21]. Thus it is assumed that the EDF in the case of a sufficiently long energy relaxation length is spatially dependent only up to a small first order correction: $F_0(\varepsilon,r)=F_0^{(0)}(\varepsilon)+F_0^{(1)}(\varepsilon,r)$. The main simplification in the nonlocal approach is achieved by the consideration of the different time scales of spatial diffusion and diffusion in energy space. In cases where the energy relaxation length is sufficiently large and the electric field is not too strong, the spatial diffusion is a much faster process than the diffusion in energy space. This fact justifies an averaging of the kinetic Eq. (4) over the cross section, which is accessible for the electrons with a certain total energy (see Fig. 3). The physical interpretation of this averaging procedure is that information acquired by the electrons, such as, for instance, heating, is distributed over the whole (accessible) cross section or in other words that every point of the cross section contributes to the formation of the EDF. The equation obtained by this averaging procedure is an ordinary differential equation for the EDF $F_0^{(0)}(\varepsilon)$:

$$\frac{d}{d\varepsilon}\left[\bar{D}_\varepsilon\frac{dF_0^{(0)}(\varepsilon)}{d\varepsilon}+\bar{V}_\varepsilon F_0^{(0)}(\varepsilon)\right]=\sum_k\left[\bar{\nu}_k^*(\varepsilon)F_0^{(0)}(\varepsilon)-\bar{\nu}_k^*(\varepsilon+u_k)F_0^{(0)}(\varepsilon+u_k)\right]+\bar{S}_{ee}\ , \tag{5}$$

with the radially averaged quantities

$$\bar{D}_\varepsilon=\frac{2e}{3m}\int_0^{r^*(\varepsilon)}u^{3/2}(r)\frac{E_p(r)^2}{2}\frac{\nu_m}{(\nu_m^2+\omega^2)}r\,dr\ , \tag{6a}$$

$$\bar{V}_\varepsilon=\frac{2m}{M_a}\int_0^{r^*(\varepsilon)}u^{3/2}(r)\nu_m(u)r\,dr\ , \tag{6b}$$

$$\bar{\nu}_k^*(\varepsilon)=\int_0^{r^k(\varepsilon)}\nu_k(u(r))\sqrt{u(r)}r dr\ . \tag{6c}$$

$r^*(\varepsilon)$ is the turning point radius (Fig. 3), $r^k(\varepsilon)$ is the maximum radius, for which the kth inelastic process is possible: $u(r^k(\varepsilon))=u_k$. $\bar{S}_{ee}$ is the radially averaged electron-electron collision integral (see Ref. [24]).

The important point is, that although obtained from the spatially averaged kinetic Eq. (5), the spatial information is fully included in the unique EDF of total energy $F_0^{(0)}(\varepsilon)$ in combination with the dc space charge potential. In fact, the distribution function of kinetic energy at a distinct radial position can be easily found from $F_0^{(0)}(\varepsilon)$

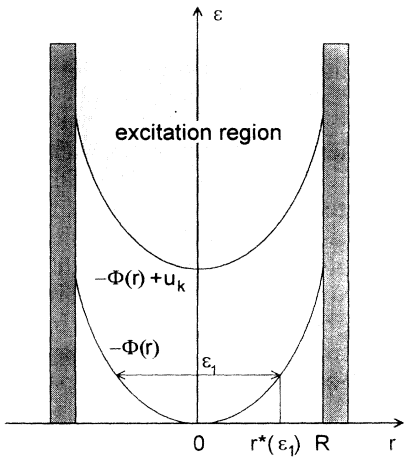

FIG. 3. Energetic conditions for confined electrons in the total-energy coordinate space according to the nonlocal model. The shaded "excitation" region marks the region where the kinetic energy is sufficient to perform exciting collisions.

by backsubstitution:

$$F_0(u,r)=F_0^{(0)}(\varepsilon=u-\Phi(r)) \ . \tag{7}$$

The meaning of this relation can be clarified by Fig. 4. At the radial position r_0 the potential energy $-\Phi(r_0)$ constitutes a threshold for the electrons. Electrons with a total energy less than this value are reflected by the space potential before reaching r_0. Electrons with a higher total energy can reach this position with their kinetic energy being $u(r_0)=\varepsilon+\Phi(r_0)<u(r=0)$. Thus $F_0(u,r_0)$ is obtained from $F_0^{(0)}(\varepsilon)$ by cutting the low energy part with $\varepsilon<-\Phi(r_0)$ and using the value $-\Phi(r_0)$ as the new zero of the kinetic energy scale. It is obvious that this procedure is the direct correspondence to the experimental results discussed in Sec. II, at least qualitatively. Thus the main assumptions of the nonlocal approach are qualitatively supported by the presented experimental results.

Additional equations are needed to complete the model. Thus the simultaneous determination of the dc space charge potential is obligatory. It can be found from a fluid approach for the ion dynamics [42] and the normalization condition for the EDF, which defines a relation between the electron density and the space charge potential [23,43]:

$$\begin{aligned} n_e(\Phi(r))&=\int_0^\infty F_0(u,r)\sqrt{u}\ du \\ &=\int_{-\Phi(r)}^\infty F_0^{(0)}(\varepsilon)\sqrt{\varepsilon+\Phi(r)}d\varepsilon \ . \end{aligned} \tag{8}$$

For the ions the continuity and momentum transport equation are used. Assuming quasineutrality ($n=n_e=n_i$) and neglecting the ion temperature in comparison to the electron "temperature," these equations read

$$\frac{1}{r}\frac{d}{dr}(rnv_r)=n\nu_i \ , \tag{9}$$

$$v_r\frac{dv_r}{dr}=-\left[\frac{e}{M_i}\frac{d\Phi}{dr}+(\nu_{in}+\nu_i)v_r\right] \ . \tag{10}$$

Here v_r is the drift velocity of the ions and M_i is the ionic mass. The ionization frequency $\nu_i=\nu_i(r)$ is calculated as an average over the distribution of kinetic energy at the radial position r with the help of Eq. (7). ν_{in} is the ion-neutral collision frequency, which is velocity dependent for rare gases due to the dominating symmetric charge exchange collision [44]:

$$\nu_{in}(v_r)=\nu_{in0}\left[1+a\frac{M_iv_r^2}{kT_g}\right]^{1/2} \ , \tag{11}$$

with $a=0.183$ a numeric constant. The method of solution of Eqs. (9) and (10) in combination with Eq. (8) is very similar to that described by Franklin [45]. As a boundary condition the Bohm criterion, that the ion drift velocity v_r has to be equal to the ion sound speed at the plasma sheath edge, has been used. For simplicity a zero sheath thickness has been assumed so that this condition has to be fulfilled exactly at the wall. The error imposed by this assumption for the value of the maintaining hf electric field is negligible. The error for the potential distribution may be important only in close vicinity of the wall.

With the density profile obtained from Eqs. (8)–(10) the hf electric field profile can also be evaluated. The method of finding the field profile has been discussed in detail elsewhere [46,47] and should therefore be sketched here only very roughly. The plasma is described by a radially dependent dielectric constant:

$$\varepsilon_p(r)=1-\frac{\omega_p^2(r)}{\omega(\omega-i\nu_c)} \ , \tag{12}$$

with $\omega_p=\omega_p(r)=[n_e(r)e^2/m_e\varepsilon_0]^{1/2}$ the radially dependent electron plasma angular frequency and ν_c the effective collision frequency for momentum transfer [48]. For simplicity ν_c has been considered as radially constant. For the case of the azimuthally symmetric surface wave mode the electromagnetic field consists of the three components E_z, E_r, and H_ϕ (z direction along the plasma axis) only. The radial profile of the E_z component is obtained from the following equation, which can be derived from the wave equation (e.g., [49,50]):

$$\frac{d^2E_z}{dr^2}+\left[\frac{1}{r}+\frac{\gamma^2}{k_m^2(r)}\frac{d\varepsilon_m(r)/dr}{\varepsilon_m(r)}\right]\frac{dE_z}{dr}+k_m^2(r)E_z=0 \ . \tag{13}$$

ε_m is the dielectric permittivity of the medium, i.e., plasma, glass, or vacuum. γ is the complex axial propagation constant of the wave. $k_m(r)$, defined by $k_m^2(r)=k_0^2\varepsilon_m(r)+\gamma^2$ with $k_0=\omega/c$ the vacuum wave number, may be considered as the radial propagation constant. γ has to be found to fulfill the continuity of E_z

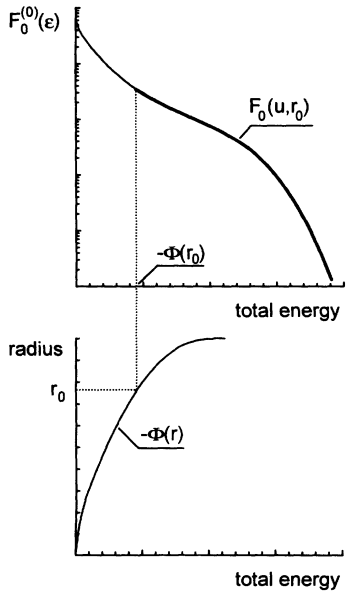

FIG. 4. Scheme for finding the EDF of kinetic energy (bold part of the curve in upper diagram) at a position r_0 from the EDF of total energy (whole curve in upper diagram) and the dc space charge potential (lower diagram).

and H_ϕ, which defines the dispersion relation of the surface wave (see, e.g., [46,47]). Having found the relative profile of E_z from Eq. (13) and the radial component from

$$E_r(r) = -\frac{\gamma}{k_p^2(r)} \frac{\partial E_z}{\partial r} , \tag{14}$$

the surface wave electric field profile in the plasma is found up to a factor E_p. The value of E_p is found as an eigenvalue of the combination of Eqs. (9) and (10).

As will become evident below, the experimental studies are performed in a pressure range where the effects of stepwise ionization may already become important. The correct treatment of the effects of excited atoms requires the use of more or less complex collisional-radiative models. However, since it is not the aim of this paper to investigate the kinetics of a specific gas, excited atoms are only taken into account in a very rough and qualitative manner in order to clarify the trends caused by their influence. Thus for all gases only the most populated metastable level is considered: the $2\,^3S$ level in helium and the $^3P_2$ levels in argon and neon. As the only population mechanism the direct excitation from the ground state is assumed. The collisional loss processes are estimated by the excitation rate to the levels of the next higher main quantum number or as simply the ionization from this level for the case of helium [51]. Furthermore, diffusion losses are accounted for, which may be important at low electron densities. The resulting population densities of these states are found by

$$n_{\rm ex} = \frac{N_0 n_{e0} \nu_0}{n_{e0}\nu_l + D_{\rm ex}/(R/2.4)^2} , \tag{15}$$

where ν_0 is the ground state excitation rate, ν_l the loss rate by excitation to higher levels or by ionization. $D_{\rm ex}$ is the diffusion coefficient of the metastable, and n_{e0} the electron density in the center. For predominant excitation losses a flat profile of the metastable atoms' density has been assumed, in the case of predominating diffusion losses a Bessel profile has been used. With these values of the excited atom densities, their contribution to the ionization can be evaluated. For $\nu_i(r)$ the sum of ground state ionization and ionization from the excited states is considered in Eqs. (9) and (10). The excited atoms are not taken into account in the collision term of the Boltzmann equation, i.e., the effect of excitation from these levels as well as the superelastic collisions are neglected in this approach. All ionization and excitation frequencies have been calculated using the cross-section material presented in [52].

Due to the great simplicity of the nonlocal model used for the electron kinetics, the whole model is easily solved on a personal computer within a few minutes of computation time. Since the profiles of the dc space charge potential and the surface wave electric field appear only in integral expressions, their exact shapes possess only minor influence on the EDF. Thus an iterative method has of the surface wave field been used to fulfill all equations simultaneously. At first, assuming some starting dc space charge potential distribution and, for instance, a flat profile of the surface wave field, the kinetic Eq. (5) is solved. The resulting dc space charge potential profile is obtained from the integration of Eqs. (8)–(10) (with or without contribution of stepwise ionization) and the electric field amplitude E_p is varied to fulfill the Bohm criterion at the position of the wall. The same procedure is repeated with the new dc space charge potential profile until a self-consistent set of EDF and potential is found. The calculation of the hf electric field profile represents the outer iteration of the algorithm.

B. Range of applicability

The range of applicability of the nonlocal approach can be found by comparing the spatially dependent first order correction $F_0^{(1)}(\varepsilon,r)$ to the spatially homogeneous main part of the EDF $F_0^{(0)}(\varepsilon)$. By inserting the expansion $F_0(\varepsilon,r) = F_0^{(0)}(\varepsilon) + F_0^{(1)}(\varepsilon,r)$ (with $F_0^{(1)} \ll F_0^{(0)}$) into Eq. (4) and by accounting for the most important terms only, one obtains

$$\left[\frac{1}{r}\frac{\partial}{\partial r}\left[rD_r(\varepsilon,r)\frac{\partial}{\partial r}F_0^{(1)}(\varepsilon,r)\right] + \frac{\partial}{\partial \varepsilon}\left[D_\varepsilon(\varepsilon,r)\frac{\partial}{\partial \varepsilon}F_0^{(0)}(\varepsilon)\right]\right] = \nu^*(\varepsilon,r)\sqrt{u(r)}F_0^{(0)}(\varepsilon) . \tag{16}$$

(Remember that ν^* denotes the total inelastic collision frequency.) The spatial and the energy diffusion coefficients are defined by

$$D_r(\varepsilon,r) = \frac{2e}{3m}\frac{u^{3/2}(r)}{\nu_m} , \tag{17}$$

$$D_\varepsilon(\varepsilon,r) = \frac{2e}{3m}\frac{u^{3/2}(r)}{\nu_m} E_{\rm eff}^2(r,u(r)) , \tag{18}$$

respectively. From Eq. (16) it is obvious that deviations from the nonlocality of the EDF may be caused by two different effects: by the heating due to the hf electric field and by energy loss due to inelastic collisions. Thus in contrast to the ideas of a local model, where a spatially constant electric field implies a spatially homogeneous EDF, even a spatially homogeneous electric field may lead to deviations from the nonlocality of the EDF. In principle the first order correction $F_0^{(1)}$ can be determined from Eq. (16) in order to verify the applicability of the nonlocal approach, i.e., that $F_0^{(1)} \ll F_0^{(0)}$. However, the range of applicability should be estimated by some simpler considerations. In the spatially averaged representation [see Eq. (5)] the heating and the inelastic loss term are essentially equal. Thus in the excitation region (the shaded region in Fig. 3), which is limited by a boundary radius $r^{\rm ex}(\varepsilon) < R$, the inelastic loss term dominates. Neglecting the heating term, Eq. (16) reduces to a one-dimensional diffusion equation. In order to obtain a sim-

ple estimate, the radial variation of $u(r)$ for a distinct ε is neglected, which is a reasonable approximation for the high total energies ε in the inelastic range of the EDF. Thus the following relation is obtained:

$$\frac{F_0^{(1)}}{F_0^{(0)}} \approx \tilde{\nu}^*(\varepsilon)\sqrt{\varepsilon}\frac{(r^{\mathrm{ex}}(\varepsilon)/2.4)^2}{D_r(\varepsilon)} \ll 1 \ . \tag{19}$$

Here $\tilde{\nu}^*(\varepsilon)$ is some typical value of the total inelastic collision frequency, which can be approximated by a cross-section averaged collision frequency. Since this criterion is particularly interesting for energies somewhat higher than the ionization threshold, where $r^{\mathrm{ex}}(\varepsilon) \approx R$ holds, relation (19) can also be formulated as

$$N_0^2(R/2.4)^2 \ll \frac{1}{3\tilde{Q}^*(\varepsilon)Q_m(\varepsilon)} \ , \tag{20}$$

where Q_m is the momentum transfer cross section and $\tilde{Q}^*$ is an effective total inelastic cross section, which accounts for the fact that $\tilde{\nu}^*(\varepsilon)$ is considerably smaller than $\nu^*(\varepsilon, r=0)$. In the following it will be approximated by $\tilde{Q}^*(\varepsilon) \approx Q^*(\varepsilon, r=0)/2$.

In the discharge regions, where the inelastic collisions are unimportant, i.e., close to the wall or in regions of a high hf field strength, the spatial diffusion has to be compared to the energy diffusion. In the same way as above, from Eq. (16) the following estimate may be derived:

$$\frac{D_r(\varepsilon)}{(R/2.4)^2}F_0^{(1)} \approx \frac{D_\varepsilon(\varepsilon)}{\varepsilon_1^2}F_0^{(0)} \ . \tag{21}$$

Using the requirement $F_0^{(1)}/F_0^{(0)} \ll 1$ one obtains

$$E_{\mathrm{eff}}^2(r, u(r)) \ll \left[2.4\frac{\varepsilon_1}{R}\right]^2 . \tag{22}$$

ε_1 is a typical energy scale for the decrease of the EDF. It may, for example, be defined as the local (in energy space) temperature of the EDF: $\varepsilon_1 = -(\partial F_0^{(0)}/\partial\varepsilon)/F_0^{(0)}$. Criterion (22) is obviously also most severe in the tail of the EDF, where the local temperature is smaller than in the elastic range of the EDF. In fact, in the tail region relations (20) and (22) coincide, since ε_1 may be approximated by $\varepsilon_1 \approx [D_\varepsilon(\varepsilon)/\tilde{\nu}^*(\varepsilon)\sqrt{\varepsilon}]^{1/2}$, as can be seen from Eq. (5).

From the above considerations the range of applicability of the nonlocal approach can be estimated. From relation (20) the following (approximate) values for the upper limit of the pressure are evaluated: for argon at $\varepsilon = 18$ eV one obtains $(pR)^2 \ll (0.2 \text{ Torr cm})^2$, for neon and helium at $\varepsilon = 30$ eV $(pR)^2 \ll (1.0 \text{ Torr cm})^2$ and $(pR)^2 \ll (1.4 \text{ Torr cm})^2$ are derived, respectively. From relation (22) the following estimates for an upper boundary of the effective field strength are obtained: 150 V/m for argon at 600 mTorr and 18 eV, 230 V/m for neon at 2 Torr and 25 eV, and 300 V/m for helium also at 2 Torr and 25 eV. For the determination of ε_1 the theoretical EDF's presented below have been used. It has to be mentioned that these are only rough estimates. In particular, the separate consideration of the inelastic losses and the energy diffusion by heating may yield too pessimistic estimates, since both effects are somewhat counterbalancing as may be seen from Eq. (16) or (5).

When the relations (19) and/or (21) are significantly violated, deviations of the nonlocality have to be expected. From the above considerations it follows that these deviations from the spatial homogeneity of the EDF should at first appear in the inelastic tail of the EDF. The EDF should transit from the nonlocal limit to the local limiting case, where the EDF is in equilibrium with the local hf electric field. For medium pressures some intermediate behavior has to be expected: a nonlocal character in the elastic range of the EDF, where the energy relaxation length is still large compared to the inhomogeneity scale, and a local character in the inelastic range, where the energy relaxation length is small. This transition from the nonlocal to the intermediate regime has been experimentally demonstrated by Godyak and Piejak [37] in a capacitively coupled rf discharge. It may be suspected, that this transition is favored by the strongly inhomogeneous rf field in this discharge.

IV. EXPERIMENTAL AND THEORETICAL RESULTS

After the more qualitative coincidence pointed out in the discussion above, a quantitative comparison between experimental and numerical results of the above model are presented in the following. In Fig. 5 experimentally determined EDF's, which have been measured at different radial positions in an argon discharge, are plotted against the total energy. It should be stressed again that the experimental EDF's are functions of the kinetic energy, but their origin is shifted according to the value of the potential energy at the corresponding position. As already discussed in connection with Fig. 2 an important experimental result, which is supported by all measurements, is that the high energy parts of the EDF's at different radial positions coincide. This is particularly evident in the energy range, in which inelastic collisions take place, for argon at energies higher than 11.55 eV. The cutting of the low energy part of the EDF when moving from the center towards the boundary is obvious for all measurements. As explained above, this observation gives strong evidence on the hypothesis that the EDF is a spatially homogeneous function of the total energy of electrons or simply on the nonlocal character of the EDF.

Moreover, also the quantitative agreement between measurements and theoretical results is convincing. The bold curves represent the theoretical results for the EDF of total energy, which corresponds to the EDF of kinetic energy in the center of the discharge, with (solid lines) and without (dashed lines) additional stepwise ionization. In comparison to the EDF's without stepwise ionization its inclusion leads to a better agreement in particular in the inelastic range of the EDF, thus giving a correction in the right direction. This behavior mirrors the well-known fact that the maintaining (hf) field strength is diminished due to the additional source of ionization. The arrows at the theoretical curves correspond to the theoretical values of the (negative) space charge potential at the corresponding radial positions, i.e., the position

where the theoretical curves have to be cut in order to find the EDF of kinetic energy. Obviously the theoretical variation of the (dc) space charge potential is slightly stronger than the one experimentally observed. However, since the EDF is only weakly dependent on the exact shape of the potential, as explained above, this deviation does not cause a strong disagreement between experimental and theoretical EDF's. The problem thus seems to be more a question of the correct calculation of the space charge potential than of the theoretical determination of the EDF. It should be remembered that the reasons for the bad coincidence of the different measured EDF's at low energies near their zeros of kinetic energy may be interpreted as experimental deficits: the limited bandwidth of the differentiating network and/or the incomplete compensation of the hf electric field. In particular, for the highest pressure of 600 mTorr the criteria (20) and (22) are slightly violated. Nevertheless, no serious deviation from the nonlocality is observed. This fact gives some indication that the rough approximations made in the deviation of relations (20) and (22) yield too severe formulations. A fact which probably favors the nonlocality of the EDF is the radially almost homogeneous hf electric field due to the relatively low frequency and electron density [47].

Figure 6 presents similar measurements for neon. Here a stable operation of the discharge is possible only for higher pressures as compared to argon. The nonlocal character of the EDF is in the same way obvious as for argon. Even for the highest pressure of 2 Torr no obvious deviation from the nonlocality arises, although this pressure is about a factor 2 higher than the maximum pressure estimated from relation (20). The comparison to the theoretical results is good only for the lowest pressure

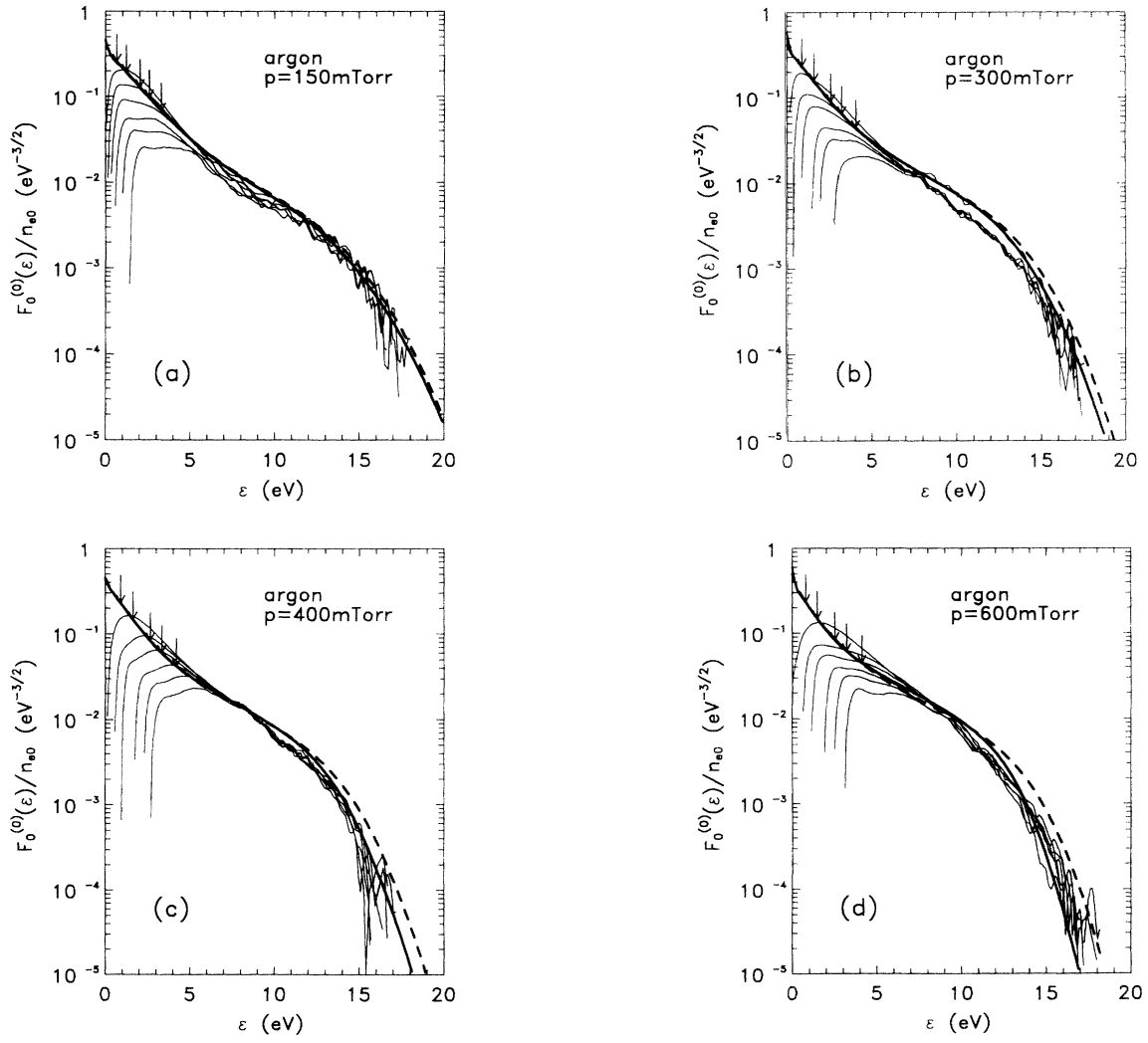

FIG. 5. Comparison between measured EDF's (of kinetic energy) at different radial positions (0, 6, 8, 10, 11, 12 mm from left to right) and theoretical results for argon. The bold solid curve represents the calculation with stepwise ionization, the bold dashed curve the one without stepwise ionization taken into account. The arrows at the theoretical curves mark the theoretical values of the potential energy at the positions 6, 8, 10, 11, and 12 mm (from left to right), i.e., the positions which correspond to the zeros of the theoretical EDF's of kinetic energy.

of 600 mTorr [Fig. 6(a)]. For higher pressures the experimental EDF's show a stronger decrease in the inelastic range than the theoretical EDF's. The calculations with the estimated inclusion of stepwise ionization yield a correction in the right direction. However, it is not astonishing, that the simple estimate for the population density does not yield the correct amount of additional stepwise ionization. The coincidence between experimental and theoretical values of the space charge potential is better than for argon.

Figure 7 depicts the same measurements in helium. These measurements show qualitatively the same behavior as for neon. The nonlocal character of the EDF is evident as for the other gases before. The deviation from theory at the higher pressure (2000 mTorr) may again be attributed to the effect of stepwise ionization. Again no obvious deviation from the nonlocality occurs even for the highest pressure.

Figure 8 exemplifies the radial variation of the dc space charge potential obtained from the probe measurements and the above model in a more illustrative manner than in Figs. 5–7. While for neon [Fig. 8(b)] (and helium, not shown here) usually good agreement is obtained, the deviations for argon [Fig. 8(a)] are more pronounced. The inclusion of the stepwise ionization tends to flatten the theoretical potential profile, thus giving the trend in the correct direction.

The mean energies determined from measured EDF's (of kinetic energy) are shown in Fig. 9. The error bars are estimated by extrapolating the measured EDF's towards zero kinetic energy in order to tentatively correct the low energy deviations of the EDF's. The general trend of a decrease of the mean energy corresponds to the fact that the EDF of kinetic energy is found from that of total energy by cutting the low energy part. Thus on the scale of kinetic energy the inelastic range of the EDF, which possesses a steeper slope [or lower "local" (in energy space) temperature] is shifted to lower values on the kinetic energy scale. Hence the decrease of the mean energy is also a direct consequence of the nonlocality of the EDF. For the mean energies in argon at first a slight increase is observed. The reason for this effect may be seen

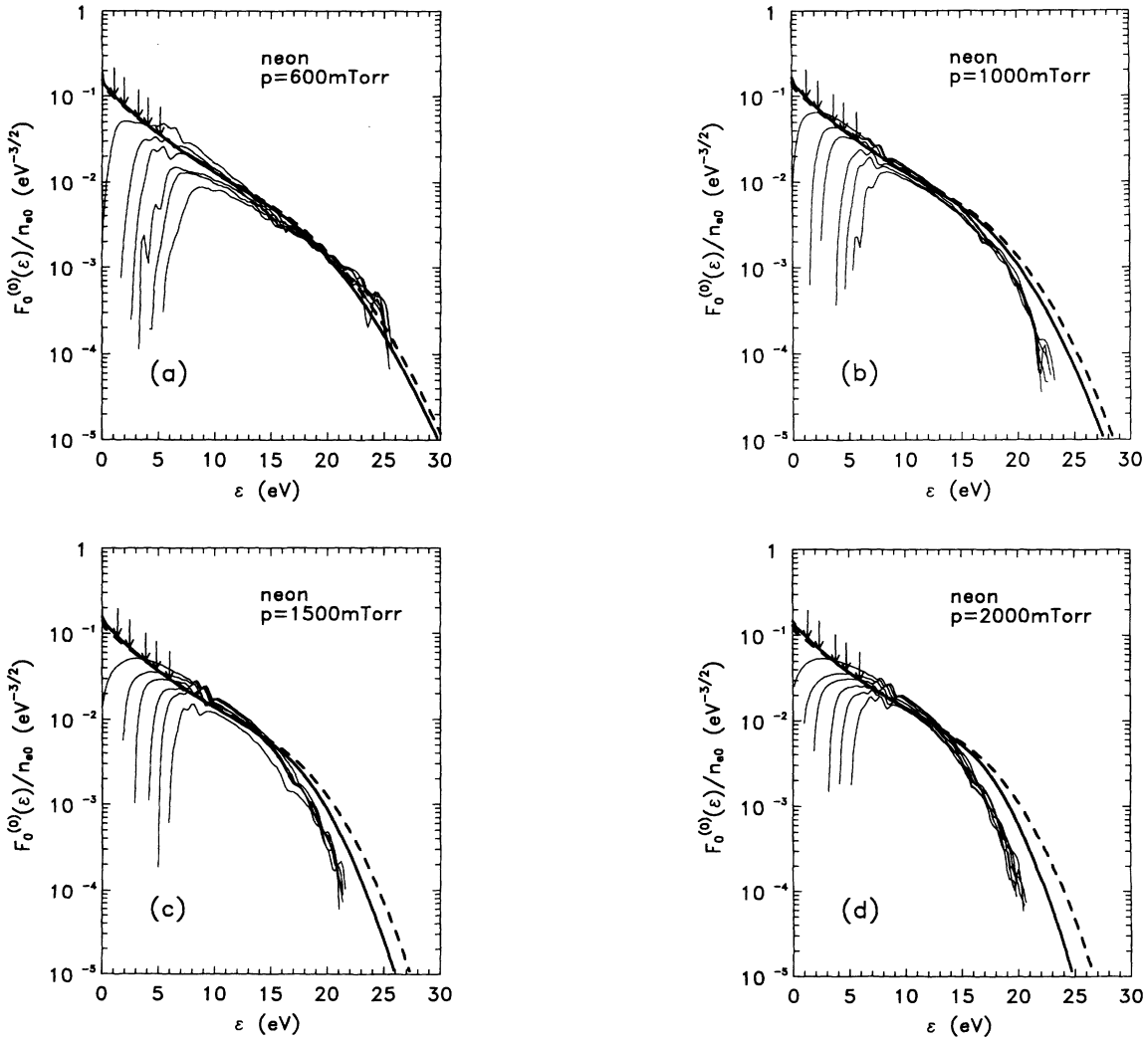

FIG. 6. Measured and theoretical results for neon in the same representation as in Fig. 5.

in the specific shape of the EDF due to the Ramsauer effect of argon and the heating by a hf electric field. As discussed elsewhere [27] the reduced collision frequency in the range near the Ramsauer minimum leads to a weak energy transfer to the electrons and thereby to a region of low "local" temperature of the EDF. Due to the cutting of the low energy part in the space charge potential this "low temperature region" of the EDF is removed, yielding the initial increase of the mean energy.

V. SUMMARY AND CONCLUSION

In the present investigation the radial dependence on the EDF in a hf plasma, sustained by a propagating surface wave, has been studied by means of a Langmuir probe diagnostic. As a result of the experimental data it has been found that the EDF can be considered as a function of the total energy (kinetic plus potential energy), which is independent of the radial position. The radial changes of the EDF of kinetic energy can be interpreted as a simple removal of low energy electrons, which do not

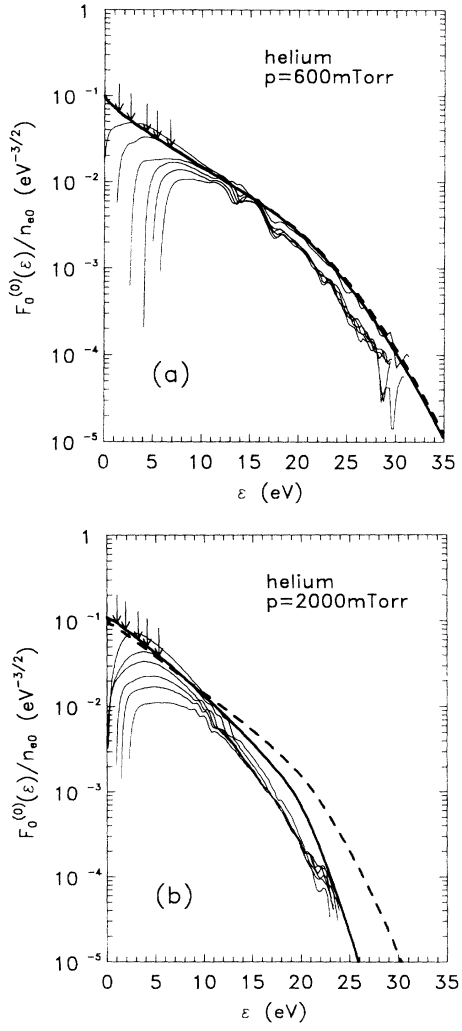

FIG. 7. Measured and theoretical results for helium in the same representation as in Fig. 5.

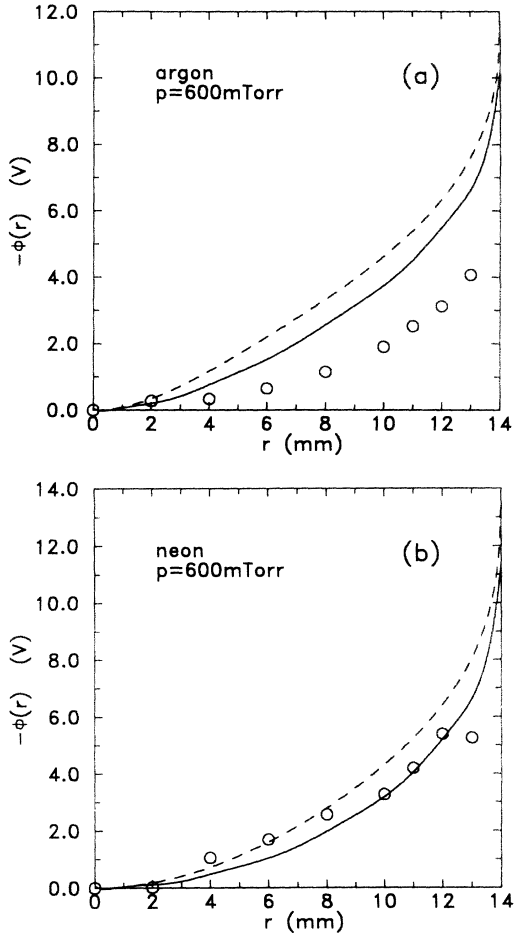

FIG. 8. Measured and theoretical profiles of the dc space charge potential for argon and neon. The circles represent the measurements, the solid lines the theoretical profiles with stepwise ionization, and the dashed lines the theoretical results without stepwise ionization taken into account.

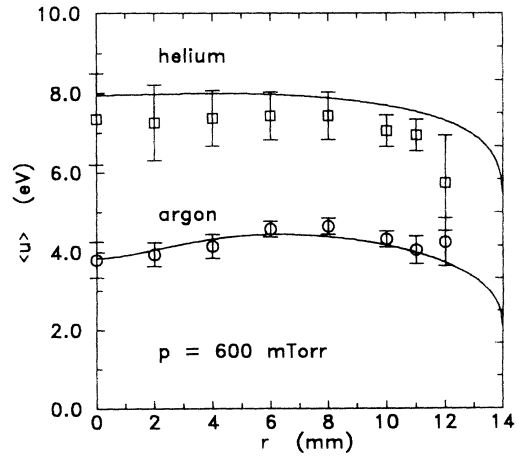

FIG. 9. Radial profiles of measured (circles) and calculated (solid lines) mean kinetic energies for argon and helium. The theoretical curves have been obtained with stepwise ionization taken into account.

possess a sufficiently high total energy to overcome the space charge potential. It has been shown that the experimental results are in close correspondence to the main ideas and assumptions of the "nonlocal approach" by Bernstein and Holstein [21] and Tsendin [22]. This approach is a significant simplification in comparison to the solution of the complete spatially inhomogeneous Boltzmann equation, since the equation is reduced by means of a spatial averaging procedure to an ordinary differential equation for the unique EDF of total energy. It has been demonstrated that the procedure of finding the EDF of kinetic energy at a spatial position from the EDF of total energy and the space charge potential is in close analogy to the experimental results. Furthermore, a quantitative comparison between the experimental results and the predictions of a (one-dimensional) discharge model, based on the nonlocal approach, has been presented. Considerable agreement has been found for argon, neon, and helium for lower pressures. The deviations at higher pressures have been attributed to the effect of stepwise ionization, which has been included in a rough manner only. Even for the highest pressures, where a stable discharge operation was possible (600 mTorr for argon, 2000 mTorr for helium and neon), no obvious deviations from the nonlocality of the EDF have been observed. In these cases the applied pressures and the theoretical values of the effective field strength exceeded the estimated upper limits for the validity of the nonlocal about a factor 2. Obviously the consideration of the applicability range deserves a more rigorous discussion. Furthermore, it has been pointed out that the nonlocality of the EDF leads to the general trend of a decrease of the mean electron energy close to the wall, where the space charge potential falls off steeply. Nevertheless, the slight increase of the mean energy observed for argon when starting from the axis of the discharge is also consistent with the nonlocal model, since the low energy part with low "local" temperature, due to the Ramsauer effect and the hf field heating, is removed by the space charge potential. Thus in fact the low energy electrons are not only localized in energy but also in coordinate space close to the discharge axis, as has also been demonstrated in [37].

The nonlocal approach must certainly be considered as an approximation, which finds its range of validity under conditions when the energy relaxation length is large compared to the discharge dimensions. Thus for higher pressures a transition to the local regime or some hybrid regime (nonlocal in the elastic energy range and local in the inelastic range) has to be expected. Exactly this transition has been observed in [37]. However, inside its range of applicability the nonlocal approach should constitute a great simplification in the description of the electron kinetics. This aspect deserves attention with respect to the modern development in the discharge modeling, in particular for models involving more than one spatial dimension. The great advantage of the nonlocal approach is that regardless of the number of spatial dimensions, the EDF is determined by a simple ordinary differential equation. Its solution can be performed with high accuracy and very limited computational efforts compared to other techniques. Of course, lots of work remains to be done. In particular, the validity of the nonlocal approach should be checked by rigorous comparison to the solution of the complete spatially inhomogeneous Boltzmann equation by different techniques and the ranges of applicability should be worked out in detail for different gases and also for electric field configurations with strong spatial inhomogeneity. These points should be left for future work.

ACKNOWLEDGMENTS

The author is grateful to Professor L. D. Tsendin for valuable discussions and for directing his interest on the subject of the nonlocal approach. The author is obliged to Professor H. Schlüter for his permanent interest in the progress of this work and for fruitful conversations. This work was supported by the Sonderforschungsbereich 191.

[1] P. M. Meijer, W. J. Goedherr, and J. D. P. Passchier, Phys. Rev. A **45**, 1098 (1992).
[2] M. J. Hartig and M. J. Kushner, J. Appl. Phys. **63**, 1080 (1993).
[3] V. A. Feoktistov, A. M. Popov, O. B. Popovicheva, A. T. Rakhimov, T. V. Rakhimova, and E. A. Volkova, IEEE Trans. Plasma Sci. **19**, 163 (1991).
[4] M. J. Kushner, J. Appl. Phys. **54**, 4958 (1983).
[5] M. J. Kushner, J. Appl. Phys. **61**, 2784 (1987).
[6] T. J. Sommerer and M. J. Kushner, J. Appl. Phys. **71**, 1654 (1992).
[7] N. Sato and H. Tagashira, IEEE Trans. Plasma Sci. **19**, 102 (1991).
[8] C. K. Birdsall, IEEE Trans. Plasma Sci. **19**, 65 (1991).
[9] M. Surendra, D. B. Graves, and I. J. Morey, Appl. Phys. Lett. **56**, 1022 (1990).
[10] M. Surendra and D. B. Graves, Appl. Phys. Lett. **59**, 2091 (1991).
[11] M. Surendra and D. B. Graves, IEEE Trans. Plasma Sci. **19**, 144 (1991).
[12] D. Vender and R. W. Boswell, IEEE Trans. Plasma Sci. **18**, 725 (1990).
[13] V. Vahedi, M. Surendra, G. DiPeso, P. Mirrashidii, and C. K. Birdsall, *1992 International Conference on Plasma Physics, Innsbruck, Austria, 1992,* edited by W. Freysinger, K. Lackner, R. Schrittwieser, and W. Lindinger (European Physics Society, Petit-Lancy, 1992), Vol. 16c, Part III, p. 1993.
[14] G. J. Parker, W. N. G. Hitchon, and J. E. Lawler, Phys. Fluids B **5**, 646 (1993).
[15] T. J. Sommerer, W. N. G. Hichton, R. E. P. Harvey, and J. E. Lawler, Phys. Rev. A **43**, 4452 (1991).
[16] T. J. Sommerer, W. N. G. Hichton, and J. E. Lawler, Phys. Rev. Lett. **63**, 2361 (1989).
[17] T. J. Sommerer, W. N. G. Hichton, and J. E. Lawler, Phys. Rev. A **39**, 6356 (1989).
[18] J. V. DiCarlo and M. J. Kushner, J. Appl. Phys. **66**, 5763 (1989).

[19] V. Vahedi, C. K. Birdsall, M. A. Liebermann, G. DiPeso, and T. D. Rognlien, Phys. Fluids B **5**, 2719 (1993).
[20] P. L. G. Ventzek, T. J. Sommerer, R. J. Hoekstra, and M. J. Kushner, Appl. Phys. Lett. **63**, 605 (1993).
[21] I. B. Bernstein and T. Holstein, Phys. Rev. **94**, 1475 (1954).
[22] L. D. Tsendin, Zh. Eksp. Teor. Fiz. **66**, 7638 (1974) [Sov. Phys. JETP **39**, 805 (1974)].
[23] I. D. Kaganovich and L. D. Tsendin, IEEE Trans. Plasma Sci. **20**, 66 (1992).
[24] U. Kortshagen, J. Phys. D **26**, 1691 (1993).
[25] J. Margot, M. Moisan, and A. Ricard, Appl. Spectrosc. **45**, 260 (1991).
[26] M. Moisan and Z. Zakrzewski, J. Phys. D **24**, 1025 (1991).
[27] U. Kortshagen, J. Phys. D **26**, 1230 (1993).
[28] T. Okuda and K. Yamamoto, J. Appl. Phys. **31**, 158 (1960).
[29] J. D. Swift and M. J. R. Schwar, *Electrical Probes for Plasma Diagnostics* (Iliffe, London, 1970).
[30] E. Berger and A. Heisen, J. Phys. D **8**, 629 (1975).
[31] N. St. J. Braithwaite, N. M. P. Benjamin, and J. E. Allen, J. Phys. E **20**, 1046 (1987).
[32] M. J. Druyvesteyn, Z. Phys. **64**, 781 (1930).
[33] V. A. Godyak, R. B. Piejak, and B. M. Alexandrovich, Phys. Rev. Lett. **68**, 40 (1992).
[34] V. A. Godyak, R. B. Piejak, and B. M. Alexandrovich, Plasma Sources Sci. Technol. **1**, 36 (1992).
[35] K. F. Schoenberg, Rev. Sci. Instrum. **49**, 1377 (1978).
[36] H. Sabadil, S. Klagge, and M. Kammeyer, Plasma Chem. Plasma Proc. **8**, 425 (1988).
[37] V. A. Godyak and R. B. Piejak, Appl. Phys. Lett. **63**, 3139 (1993).
[38] K. Wiesemann, Ann. Phys. (Leipzig) **23**, 275 (1969).
[39] D. Hermann, A. Rutscher, and S. Pfau, Beitr. Plasmaphys. **10**, 75 (1970).
[40] I. P. Shkarofsky, T. W. Johnston, and M. P. Bachynski, *The Particle Kinetics of Plasmas* (Addison-Wesley, Reading, MA, 1966).
[41] R. Winkler, H. Deutsch, J. Wilhelm, and Ch. Wilke, Beitr. Plasmaphys. **24**, 303 (1984).
[42] S. A. Self and H. N. Ewald, Phys. Fluids **9**, 2486 (1966).
[43] L. D. Tsendin and Yu. B. Golubovskij, Zh. Tekh. Fiz. **47**, 1839 (1977) [Sov. Phys. Tech. Phys. **22**, 1066 (1977)].
[44] V. Martisovits, J. Phys. B **3**, 850 (1970).
[45] R. N. Franklin, *Plasma Phenomena in Gas Discharges* (Clarendon, Oxford, 1976).
[46] A. Granier, C. Boisse-Laporte, P. Leprince, J. Marec, and P. Nghiem, J. Phys. D **20**, 204 (1987).
[47] M. Zethoff and U. Kortshagen, J. Phys. D **25**, 1574 (1992).
[48] R. K. Whitmer and G. F. Herrmann, Phys. Fluids **9**, 768 (1966).
[49] M. Moisan, R. Pantel, A. Ricard, V. M. M. Glaude, P. Leprince, and W. P. Allis, Rev. Phys. Appl. **15**, 1383 (1980).
[50] C. M. Ferreira, J. Phys. D **14**, 1811 (1981).
[51] P. A. Miller, J. T. Verdeyen, and B. E. Cherrington, Phys. Rev. A **4**, 692 (1971).
[52] J. Krenz, Inst. Plasmaphys. Univ. Hannover, BMFT Project Report No. 13N54069, 1987 (unpublished).

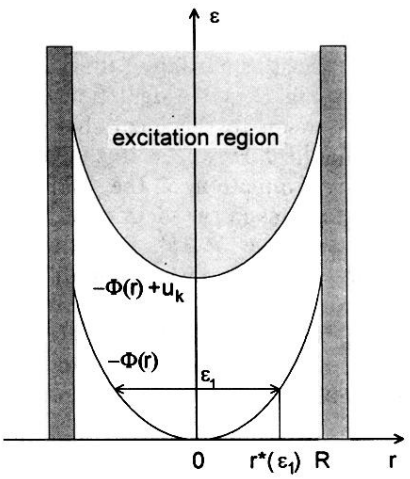

FIG. 3. Energetic conditions for confined electrons in the total-energy coordinate space according to the nonlocal model. The shaded "excitation" region marks the region where the kinetic energy is sufficient to perform exciting collisions.